

Article

# Calculation of Low-Energy Positron-Atom Scattering with Square-Integrable Wavefunctions

Sarah Gregg \*  and Gleb Gribakin 

School of Mathematics and Physics, Queen's University Belfast, Belfast BT7 1NN, UK; g.gribakin@qub.ac.uk

\* Correspondence: sgregg07@qub.ac.uk

**Abstract:** The variational method is applied to the low-energy positron scattering and annihilation problem. The ultimate aim of the investigation is to find a computationally economical way of accounting for strong electron–positron correlations, including the effect of virtual positronium formation. The method is applied to the study of elastic *s*-wave positron scattering from a hydrogen atom. A generalized eigenvalue problem is set up and solved to obtain *s*-wave positron–hydrogen scattering phase shifts within  $8 \times 10^{-3}$  rad of accepted values. This is achieved using a small number of terms in the variational wavefunction; in particular, only nine terms that depend on the electron–positron distance are included. The annihilation parameter  $Z_{\text{eff}}$  is also calculated and is found to be in good agreement with benchmark calculations.

**Keywords:** theoretical atomic and molecular physics; positron; hydrogen; annihilation; phase shift; scattering



**Citation:** Gregg, S.K.; Gribakin, G.F. Calculation of Low-Energy Positron-Atom Scattering with Square-Integrable Wavefunctions. *Atoms* **2022**, *10*, 97. <https://doi.org/10.3390/atoms10040097>

Academic Editor: Yew Kam Ho

Received: 1 September 2022

Accepted: 18 September 2022

Published: 22 September 2022

**Publisher's Note:** MDPI stays neutral with regard to jurisdictional claims in published maps and institutional affiliations.



**Copyright:** © 2022 by the authors. Licensee MDPI, Basel, Switzerland. This article is an open access article distributed under the terms and conditions of the Creative Commons Attribution (CC BY) license (<https://creativecommons.org/licenses/by/4.0/>).

## 1. Introduction

The aim of this paper is to explore a numerically frugal method of including important electron–positron correlations in the calculations of positron ( $e^+$ ) scattering from atoms and molecules. A good understanding of positron interactions with matter is a crucial element in the development of current and future applications of antimatter [1,2]. It is also important for tests of quantum electrodynamics [3] and fundamental experiments with antihydrogen [4].

Since the prediction [5] and discovery [6] of the positron's existence, many experimental and theoretical studies have been focussed on revealing the nature of its interactions with atoms and molecules [7]. Measurements and calculations show that low-energy positron interaction with atoms and molecules is characterized by strong electron–positron correlations. The first of these correlation effects is polarization of the target electron distribution by the positron. It gives rise to the attractive polarization potential with the asymptotic form  $-\alpha e^2/2r^4$ , where  $\alpha$  is the dipole polarizability of the target,  $e$  is the charge of the projectile (positron), and  $r$  is the distance between the positron and the target. This polarization potential is similar to that which affects electron scattering.

The second correlation effect, which is specific to positrons, is *virtual positronium formation*. Positronium (Ps) is a light hydrogen-like atom that consists of an electron and a positron. Ps has a binding energy of  $E_{\text{Ps}} = 6.8$  eV. For positron energies  $\varepsilon > E_I - E_{\text{Ps}}$ , where  $E_I$  is the ionization energy of the target, Ps formation is an important ionization channel in positron collisions. For targets with  $E_I > E_{\text{Ps}}$  and  $\varepsilon < E_I - E_{\text{Ps}}$ , the Ps formation channel is closed. However, atomic electrons can still tunnel from an atom or molecule to the positron to form a Ps-like state temporarily. This effect makes a distinct and sizeable attractive contribution to the interaction of low-energy positrons with atoms and molecular targets. At the same time, this contribution makes positron scattering and annihilation calculations particularly challenging.

Amusia and co-workers [8] were probably the first to recognize the importance of virtual Ps formation. They were able to incorporate this effect and gauge its magnitude using

many-body theory calculations for He. (Very recently, this approach was used for positron scattering from atoms with half-filled valence shells [9].) A more accurate approximation for the Ps formation contribution to the positron–atom correlation potential [10] enabled predictions of positron binding to neutral atoms [11] and reliable calculations of positron scattering from noble gas atoms [12]. Ultimately, a consistent *ab initio* method for calculating the Ps formation contribution was developed and tested [13]. It provided a complete and accurate picture of positron scattering and annihilation from noble-gas atoms [14], and has now been generalized to molecular calculations that can yield high-quality predictions of positron–molecule binding energies [15].

Many-body theory allows one to identify the virtual Ps formation contributions with a particular class of diagrams that contribute to the positron–target correlation potential. When other approaches are used, the physical effect of virtual Ps formation is still present, but it manifests itself in a different way. In single-center convergent close-coupling calculations of positron scattering from hydrogen, one observes it as slow convergence with respect to the maximum orbital momentum of the electron and positron states used [16]. This is also seen in configuration–interaction calculations of positron–atom bound states [17]. Such high-angular-momentum states are needed to describe an electron–positron pair (Ps) localized some distance away from the atomic nucleus. This “problem” is immediately removed, however, when a two-center approach is used, in which functions that depend on the electron–positron distance (and hence, describe Ps) are included in the expansion of the wavefunction [18]. It was also seen in Kohn-variational calculations [19,20] that the inclusion of such “virtual Ps” terms in the wavefunction yields significant improvements in the convergence of the scattering phase shifts and a pronounced enhancement of the positron annihilation rate at energies just below the Ps formation threshold. Finally, when the Schwinger multichannel method is used for positron scattering from molecules [21], calculations are significantly improved by adding basis states on extra centers placed away from the atomic nuclei [22]. In this case, such centers help to describe Ps formed virtually outside the molecule. Such “ghost” centers are also used in the most sophisticated many-body theory calculations of positron–molecule binding to enable the accurate description of virtual Ps formation [15].

It can be seen from the above that a well-converged positron scattering calculation should either include a large number of wavefunction terms centered on the nuclei or include terms with explicit dependence on the electron–positron distance. The first approach is more straightforward numerically but may lead to very large basis sizes. The second one is more economical but with an added complexity of dealing with a multicenter problem. It is the latter approach that we want to explore, aiming to include as few correlation terms as strictly necessary to obtain good-quality scattering and annihilation data.

In this paper, the scattering and annihilation of positrons is explored for the positron–hydrogen system through use of the variational method with square-integrable trial wavefunctions. Important correlation effects, including that of virtual Ps formation, are accounted for by including functions which depend on the electron–positron distance. The variational method is set up as a generalized eigenvalue problem. From this, elastic *s*-wave phase shifts  $\delta$  and the annihilation parameter  $Z_{\text{eff}}$  for the  $e^+$ -H system are calculated at energies below the Ps formation threshold. Good agreement with benchmark values of both the phase shifts [23–25] and the annihilation parameter [26] is achieved using only a small number of terms in the wavefunction. By providing evidence that this method is a valid approach to the problem, avenues for future research are opened in which more complex matter–antimatter interactions may be explored. It should be added that the positron–hydrogen system has long been used as a testbed for various calculation methods, with many accurate results available at both low and high energies (see, e.g., Refs. [27–29]).

The paper is structured as follows. In Section 2, we set up the generalized eigenvalue problem which is employed to solve the scattering problem and show how to obtain the scattering phase shifts from bound-state calculations. In Section 3, the method is applied to elastic *s*-wave scattering of a positron from a hydrogen atom. Three sets of phase shift

results are presented, beginning with a simple model and progressing toward more detailed descriptions of the system. In Section 4, the annihilation parameter  $Z_{\text{eff}}$  is calculated using the same trial wavefunctions as in Section 3. Section 5 summarizes the work and indicates its future applications.

## 2. Scattering as a Bound-State Problem

In this section, we recap how a simple variational method can be used to calculate  $s$ -wave elastic scattering phase shifts for scattering from an atomic target.

### 2.1. Generalized Eigenvalue Problem

The method begins with the choice of a trial wavefunction. Consider a system in the state  $|\Psi\rangle$  expanded in terms of a set of linearly independent square-integrable basis functions  $\{|\varphi_i\rangle\}_{i=1}^N$  which, in general, are neither normalized nor orthogonal:

$$|\Psi\rangle = \sum_{i=1}^N c_i |\varphi_i\rangle. \tag{1}$$

This basis is chosen at the beginning of the problem, and the coefficients  $c_i$  are the variational parameters.

Central to the problem is the minimization of the energy functional,

$$\langle E \rangle = \langle \Psi | \hat{H} | \Psi \rangle, \tag{2}$$

with respect to the parameters  $c_i$ , whilst holding  $\langle \Psi | \Psi \rangle = 1$ . The minimum energy calculated using a trial wavefunction provides an upper bound on the exact ground-state energy of the system.

The normalization constraint is imposed during the minimization through use of a Lagrange multiplier  $E$ . At the minimum (or a stationary point), we require

$$\frac{\partial}{\partial c_k} [\langle \Psi | \hat{H} | \Psi \rangle - E(\langle \Psi | \Psi \rangle - 1)] = 0, \quad k = 1, \dots, N. \tag{3}$$

Substituting the expansion of  $|\Psi\rangle$  from (1) into (3) gives a system of  $N$  linear equations. Assuming that the  $c_i$  values are independent of each other, performing partial differentiation with respect to a particular  $c_k$  yields the following:

$$\sum_j c_j \langle \varphi_k | \hat{H} | \varphi_j \rangle + \sum_i c_i \langle \varphi_i | \hat{H} | \varphi_k \rangle - E \left( \sum_j c_j \langle \varphi_k | \varphi_j \rangle + \sum_i c_i \langle \varphi_i | \varphi_k \rangle \right) = 0. \tag{4}$$

Since the matrix elements of the Hamiltonian are real (assuming real basis functions  $|\varphi_i\rangle$ ), the first two sums in (4) are identical and hence may be combined. Similarly, the scalar product of any two basis functions in our problem is real, and the second pair of sums may also be combined. This results in the following equation:

$$\sum_i \underbrace{\langle \varphi_k | \hat{H} | \varphi_i \rangle}_{H_{ki}} c_i = E \sum_i \underbrace{\langle \varphi_k | \varphi_i \rangle}_{Q_{ki}} c_i, \tag{5}$$

where  $H_{ki}$  and  $Q_{ki}$  are the elements of matrices  $\mathbf{H}$  and  $\mathbf{Q}$ , respectively. Hence, (5) takes the form of a matrix equation:

$$\mathbf{H}\mathbf{c} = E\mathbf{Q}\mathbf{c}, \tag{6}$$

where the vector  $\mathbf{c}$  contains the  $c_i$  values.

The eigenvalues  $E_n$  of the generalized eigenvalue problem (6) are energy eigenvalues of the system with Hamiltonian  $\hat{H}$ , with the state  $|\Psi\rangle$  defined by coefficients  $c_i$ , i.e., the elements of the corresponding eigenvector. For a system that has a few bound states or no

bound states at all, most of the energy eigenvalues will lie in the continuum. The corresponding states  $|\Psi\rangle$ , often called *pseudostates*, will not be the true states of the system that represent scattering states. However, it is possible to use the energies and wavefunctions of the pseudostates to determine important properties of the scattering states, e.g., phase shifts or (for positrons) the normalized annihilation rate  $Z_{\text{eff}}$ .

In this work, the generalized eigenvalue problem is solved using Python's `eigh` function [30] which, given matrices  $H$  and  $Q$ , provides the energy eigenvalues and normalized eigenvectors of the system.

## 2.2. Scattering Phase Shifts

Once the energy eigenvalues have been calculated, they can be used to find the phase shifts  $\delta$ , e.g., for  $s$ -wave scattering. This assumes that the target is spherically symmetric and states  $|\Psi\rangle$  have zero total angular momentum. The method used by Gribakin and Swann in [31] is implemented here. Firstly, the eigenvalue problem is solved for a free particle, i.e., using a chosen basis-state expansion but neglecting the interaction between the projectile and the target in  $\hat{H}$ . The free-particle energy eigenvalues are denoted  $E_n^{(0)}$  and increase monotonically with  $n$ . Hence, it is possible to introduce an invertible function  $f(n)$  such that

$$f(n) = E_n^{(0)} \quad (7)$$

for  $n = 1, \dots, N$ . Next, the eigenvalue problem is solved with the full Hamiltonian using the same basis. The corresponding eigenvalues  $E_n$  are shifted with respect to those in equation (7), which can be written as

$$E_n = f\left(n - \frac{\delta}{\pi}\right), \quad (8)$$

where  $\delta$  is the phase shift [31].

Rearranging (8), the phase shifts may be extracted as a function of the energy eigenvalues  $E_n$ :

$$\delta = \left[n - f^{-1}(E_n)\right]\pi. \quad (9)$$

With the introduction of a phase shift  $\delta$ , the function  $f(n)$  must now be defined for real values of  $n$ , and equivalently, its inverse must be defined for values of energy other than the free-particle energy eigenvalues. The value of  $f^{-1}(E)$  for these intermediate values of energy may be found by interpolating between the free-particle energy eigenvalues. However, for particular bases, e.g., those using even-tempered exponents, the function  $f(n)$  varies rapidly and is difficult to interpolate accurately. In this case, a new function  $g(\ln E)$  can be defined, such that  $f^{-1}(E) \equiv g(\ln E)$ ; this function changes more slowly, making accurate interpolation possible. In the problems that follow, this interpolation is completed using a cubic spline fit to the data for integer  $n$ . The phase shift may then be calculated as

$$\delta = [n - g(\ln E_n)]\pi. \quad (10)$$

In the following analysis, the phase shift will be considered as a function of momentum  $k = \sqrt{2E}$  rather than energy  $E$ , where we use atomic units and assume that the projectile (positron) has a unit mass and set  $E = 0$  at the continuum threshold.

## 3. Calculation of Elastic $s$ -Wave Positron–Hydrogen Phase Shifts

In this section, the variational method is used to calculate elastic scattering phase shifts for a positron scattering from a hydrogen atom. The calculation is restricted to  $s$ -wave scattering which dominates at low positron energies.

### 3.1. One-Particle Problem

To test the method, we consider the simple problem of positron scattering from a “frozen” hydrogen atom. In this case, the wavefunction depends only on the distance between the positron and the nucleus. Figure 1 contains a schematic diagram of the system with the interparticle distances labeled.

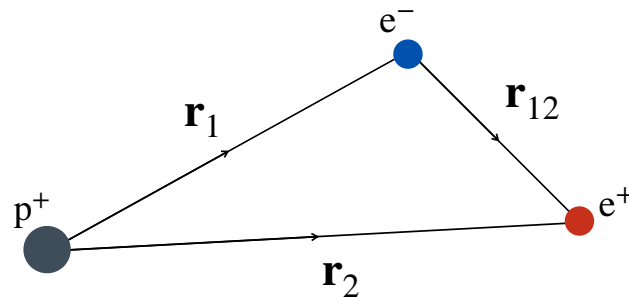


Figure 1. A diagram of the positron–hydrogen system with the interparticle distances labeled.

In the frozen-target approximation, the electron moves in the field of the nucleus (considered infinitely massive) and is “fixed” in the ground (1s) state of the atom. The dependence of the wavefunction on  $r_{12}$  is neglected. Hence, the total wavefunction becomes a product of the 1s electron wavefunction and the unknown positron wavefunction, which we denote  $\Psi(r)$ , with  $r \equiv r_2$ . Considering  $\Psi(r)$  as the wavefunction of the radial motion, the boundary condition at the origin  $\Psi(0) = 0$  is imposed. In this problem, we select a trial wavefunction of the form

$$\Psi(r) = r \sum_{i=1}^N c_i \exp(-\beta_i r), \tag{11}$$

where  $c_i$  are variational parameters and  $\beta_i$  are chosen real exponents. The corresponding basis functions are

$$\varphi_i(r) = r \exp(-\beta_i r), \quad i = 1, \dots, N. \tag{12}$$

In the following calculations, the exponents  $\beta_i$  are chosen as

$$\beta_i = \beta_1 \zeta^{i-1}, \quad i = 1, \dots, N, \tag{13}$$

i.e., forming an even-tempered basis, with  $\zeta = 1.5$ ,  $N = 20$  and  $\beta_1 = 0.01$ .

The elements of matrix  $Q$  are calculated as follows:

$$Q_{ij} = \int_0^\infty \varphi_i(r) \varphi_j(r) dr = \frac{2}{(\beta_i + \beta_j)^3}. \tag{14}$$

Next, the Hamiltonian for the system is considered<sup>1</sup>. The electrostatic potential of the ground-state hydrogen atom is (see, e.g., Ref. [32], §36, Problem 2):

$$\hat{U} = \frac{1}{r} + \phi_e(r) = \left(\frac{1}{r} + 1\right) e^{-2r}, \tag{15}$$

where  $\phi_e(r)$  is the mean-field potential of the electron cloud and the  $1/r$  term accounts for the positron-nucleus interaction.

In addition to  $\hat{U}$ , the Hamiltonian of the radial motion of the positron contains its kinetic energy, hence

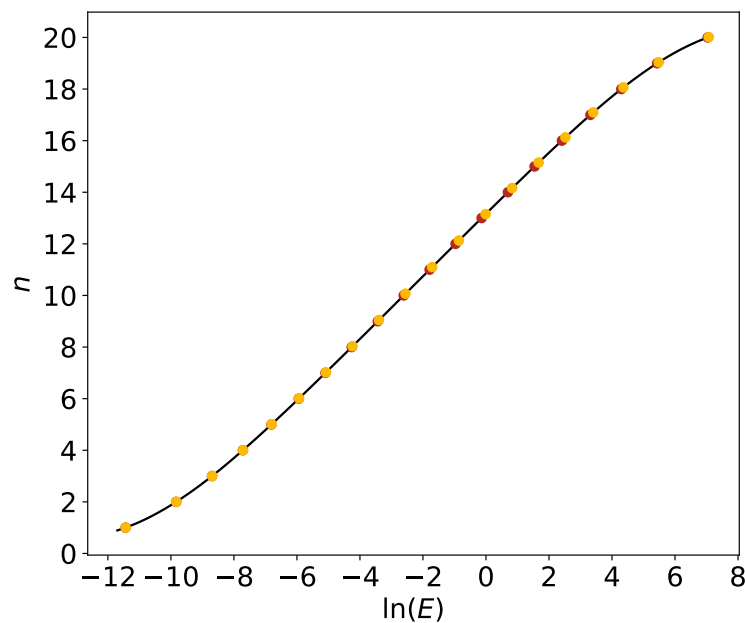
$$\hat{H} = -\frac{1}{2} \frac{d^2}{dr^2} + \left(\frac{1}{r} + 1\right) e^{-2r}. \tag{16}$$

The Hamiltonian matrix elements are calculated as follows:

$$\begin{aligned}
 H_{ij} &= \int_0^\infty \varphi_i(r) \left( -\frac{1}{2} \frac{d^2 \varphi_j(r)}{dr^2} \right) dr + \int_0^\infty \varphi_i(r) \left( \frac{1}{r} + 1 \right) e^{-2r} \varphi_j(r) dr, \\
 &= -\frac{1}{2} \frac{\beta_i \beta_j}{(\beta_i + \beta_j)^3} + \frac{\beta_i + \beta_j + 4}{(\beta_i + \beta_j + 2)^3}.
 \end{aligned}
 \tag{17}$$

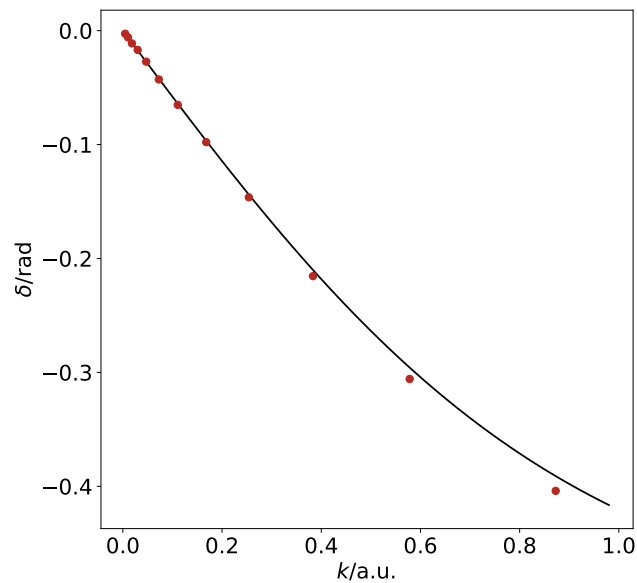
The generalized eigenvalue problem (6) for the matrices (14) and (17) was then solved using a simple Python code, and the phase shifts were calculated as described in Section 2.2.

Figure 2 is a plot of  $n$  against  $\ln E$  for the basis (13). It explains how the phase shifts are found from the pseudostate energy eigenvalues. By construction, for the free-positron eigenvalues  $E_n^{(0)}$  (obtained using  $\hat{H} = -\frac{1}{2}d^2/dr^2$ ), the function  $g(\ln E_n^{(0)})$  takes integer values, but for the eigenvalues  $E_n$  of the positron in the static hydrogen potential, this function takes non-integer values  $n - \delta/\pi$ , which yield  $\delta$  for specific positron energies  $E_n$ .



**Figure 2.** Red circles: values of  $n = 1, 2, \dots$  plotted against  $\ln E_n^{(0)}$ . Black line: the function  $n = g(\ln E)$  obtained using cubic-spline interpolation between the free-particle eigenvalue data. Yellow circles: the points on the interpolated curve for the positron energies  $E_n$  in the static hydrogen potential. From this, it can be seen that  $\ln E_n$  corresponds to non-integer ordinates  $n - \delta/\pi$ .

The phase shifts for low-momentum positrons were compared to those obtained from a numerical solution of the radial Schrödinger equation in the static hydrogen potential (obtained using the codes described in [33]). This comparison is displayed in Figure 3. There is a good agreement between these sets of data, especially at low momenta  $k$ , providing evidence that the present variational method allows one to extract the scattering phase shifts from a simple bound-state calculation.



**Figure 3.** Positron–hydrogen *s*-wave scattering phase shifts in the static approximation. Red data points: phase shifts obtained using the present variational method. Black line: data obtained by solving the radial Schrödinger equation using the suite of codes described in [33].

### 3.2. Two-Particle Problem

In this section, a full two-particle dynamics of positron scattering from a hydrogen atom is considered. Here, the electron is no longer fixed in the 1s state of the hydrogen atom and generally, the wavefunction for this system will depend on the distances between all three pairs of particles<sup>2</sup>, as labeled in Figure 1. A wavefunction of the following form will be considered:

$$\Psi(r_1, r_2, r_{12}) = \sum_{i=1}^N c_i \exp(-\alpha_i r_1 - \beta_i r_2 + \gamma_i r_{12}), \tag{18}$$

where the values of coefficients  $\alpha_i$ ,  $\beta_i$  and  $\gamma_i$  are chosen and the constants  $c_i$  are the variational parameters. The integrals to be evaluated in this section are greatly simplified by using the elliptic (Hylleraas [34]) coordinate system ( $s = r_1 + r_2, t = r_1 - r_2, u = r_{12}$ ), so these coordinates are employed to carry out all of the calculations. The full set of standard integrals used is found in Appendix A. Our calculations begin with a simplified version of (18) using a single value of  $\alpha_i = 1$  and  $\gamma_i = 0$ , i.e., equivalent to the frozen-target approximation of Section 3.1, gradually building toward the more general case. With each added element of flexibility in the wavefunction, a more accurate solution to the scattering problem is obtained.

Labeling the basis functions

$$\varphi_i(r_1, r_2, r_{12}) = \exp(-\alpha_i r_1 - \beta_i r_2 + \gamma_i r_{12}), \tag{19}$$

elements of the overlap matrix  $Q$  are calculated as follows:

$$Q_{ij} = \int \varphi_i \varphi_j d\tau, \tag{20}$$

where  $d\tau = \pi^2(s^2 - t^2)uds dt du$  is the volume element, and the integration is over  $0 \leq s < \infty, 0 \leq u \leq s, -u \leq t \leq u$ . Substituting  $\varphi_i$  from (19) into (20), we find the overlap integral in the form

$$Q_{ij} = \int \exp[2(-A_{ij}s - B_{ij}t + \Gamma_{ij}u)] d\tau, \tag{21}$$

where

$$A_{ij} = \frac{1}{4}(\alpha_i + \beta_i + \alpha_j + \beta_j), \tag{22}$$

$$B_{ij} = \frac{1}{4}(\alpha_i - \beta_i + \alpha_j - \beta_j), \tag{23}$$

$$\Gamma_{ij} = \frac{1}{2}(\gamma_i + \gamma_j). \tag{24}$$

This integral shares its structure with the standard integral  $\tilde{I}_1$  from Appendix A; hence,

$$Q_{ij} = \tilde{I}_1(A_{ij}, \Gamma_{ij}, B_{ij}). \tag{25}$$

The Hamiltonian operator of the system is given by

$$\hat{H} = -\frac{1}{2}\nabla_1^2 - \frac{1}{2}\nabla_2^2 - \frac{1}{r_1} + \frac{1}{r_2} - \frac{1}{r_{12}}. \tag{26}$$

The first two terms represent the kinetic energy of the electron and positron  $\hat{T}$ . The third and fourth terms describe the interaction of the electron and positron with the nucleus  $\hat{U}$ , and the final term represents the electron–positron interaction  $\hat{V}$ . Hence, the Hamiltonian matrix element  $H_{ij}$  is considered as the sum of three contributions:

$$H_{ij} = T_{ij} + U_{ij} + V_{ij}. \tag{27}$$

In the elliptic coordinates, the expectation value of the kinetic energy takes the form

$$\begin{aligned} \langle \Psi | \hat{T} | \Psi \rangle = \int \left\{ \left( \frac{\partial \Psi}{\partial s} \right)^2 + \left( \frac{\partial \Psi}{\partial t} \right)^2 + \left( \frac{\partial \Psi}{\partial u} \right)^2 \right. \\ \left. + \frac{2}{u(s^2 - t^2)} \frac{\partial \Psi}{\partial u} \left[ s(u^2 - t^2) \frac{\partial \Psi}{\partial s} + t(s^2 - u^2) \frac{\partial \Psi}{\partial t} \right] \right\} d\tau. \end{aligned} \tag{28}$$

Replacing one of the  $\Psi$  by  $\phi_i$  and the other by  $\phi_j$ , and mapping the integrals that arise to the set of standard integrals in Appendix A, one obtains

$$\begin{aligned} T_{ij} = \frac{1}{4} [(\alpha_i + \beta_i)(\alpha_j + \beta_j) + (\alpha_i - \beta_i)(\alpha_j - \beta_j) + 4\gamma_i\gamma_j] \tilde{I}_1(A_{ij}, \Gamma_{ij}, B_{ij}) \\ - \gamma_i [(\alpha_j + \beta_j) \tilde{I}_2(A_{ij}, \Gamma_{ij}, B_{ij}) + (\alpha_j - \beta_j) \tilde{I}_3(A_{ij}, \Gamma_{ij}, B_{ij})]. \end{aligned} \tag{29}$$

The matrix element of the electron and positron interaction with the nucleus is

$$U_{ij} = \int \phi_i \left[ -\frac{2}{s+t} + \frac{2}{s-t} \right] \phi_j d\tau. \tag{30}$$

This integral is reduced to the standard integrals  $\tilde{J}_1$  and  $\tilde{J}_3$  (Appendix A), which gives

$$U_{ij} = -2[\tilde{J}_1(A_{ij}, \Gamma_{ij}, B_{ij}) - \tilde{J}_3(A_{ij}, \Gamma_{ij}, B_{ij})] + 2[\tilde{J}_1(A_{ij}, \Gamma_{ij}, B_{ij}) + \tilde{J}_3(A_{ij}, \Gamma_{ij}, B_{ij})]. \tag{31}$$

Clearly, the  $\tilde{J}_1$  terms will cancel here. However, when calculating the free-positron energy eigenvalues, only the first bracketed term on the right-hand side of this equation is required, since the positron–nucleus interaction (second term) is not included in the free-positron Hamiltonian. When both of the Coulomb terms are included, the expression simplifies to

$$U_{ij} = 4\tilde{J}_3(A_{ij}, \Gamma_{ij}, B_{ij}). \tag{32}$$

Lastly, the matrix element of the electron–positron Coulomb interaction is given by

$$V_{ij} = - \int \varphi_i \frac{1}{u} \varphi_j d\tau. \tag{33}$$

This integral reduces to the standard integral  $\tilde{J}_2$  in Appendix A to give

$$V_{ij} = -\tilde{J}_2(A_{ij}, \Gamma_{ij}, B_{ij}). \tag{34}$$

Combining the results in (29), (32) and (34), an expression for the Hamiltonian matrix element is obtained:

$$\begin{aligned} H_{ij} = & \frac{1}{4} [(\alpha_i + \beta_i)(\alpha_j + \beta_j) + (\alpha_i - \beta_i)(\alpha_j - \beta_j) + 4\gamma_i\gamma_j] \tilde{I}_1(A_{ij}, \Gamma_{ij}, B_{ij}) \\ & - \gamma_i [(\alpha_j + \beta_j)\tilde{I}_2(A_{ij}, \Gamma_{ij}, B_{ij}) + (\alpha_j - \beta_j)\tilde{I}_3(A_{ij}, \Gamma_{ij}, B_{ij})] \\ & + 4\tilde{J}_3(A_{ij}, \Gamma_{ij}, B_{ij}) - \tilde{J}_2(A_{ij}, \Gamma_{ij}, B_{ij}). \end{aligned} \tag{35}$$

Note that for  $\gamma_i \neq 0$ , the matrix element (35) derived using equation (28) is not symmetric, i.e.,  $H_{ij} \neq H_{ji}$ . Hence,  $H_{ij}$  must be replaced by the symmetrized combination

$$H'_{ij} = \frac{1}{2}(H_{ij} + H_{ji}), \tag{36}$$

before solving the generalized eigenvalue problem (6), which is consistent with the derivation in Section 2.1.

After setting up the Hamiltonian and overlap matrices, the generalized eigenvalue problem (6) is solved for the energy eigenvalues and eigenvectors. The eigenvalues for the free positron (omitting the positron–nucleus and positron–electron interaction terms) and those for the full Hamiltonian are analyzed to extract the phase shifts, as outlined in Section 2.2. It is noted here that solving (6) provides energy eigenvalues of the whole system. Hence, to obtain the positron energies  $E_n^{(0)}$  and  $E_n$ , the energy of the ground-state hydrogen atom (−0.5 a.u.) must be subtracted from the eigenvalues.

### 3.2.1. Reproducing the Frozen-Target Results.

In the first instance, the frozen-target problem is revisited to check that the two-particle code produces the same results as the one-particle code. The dependence of the wavefunction on  $r_{12}$  is eliminated by setting  $\gamma_i = 0$ . In addition, the electron is fixed in the ground state by setting  $\alpha_i = 1$ . These restrictions will subsequently be lifted to allow the electron to move and to account for the electron–positron correlations. As before, describing the positron requires a wide range of exponents  $\beta_i$ , which are defined as in (13).

Taking all of this into account, we have the following wavefunction:

$$\Psi(r_1, r_2) = \sum_{i=1}^N c_i \exp[-r_1 - \beta_i r_2]. \tag{37}$$

Figure 4 shows that the corresponding phase shifts match those from the one-particle problem 3.1. Figure 4 also shows the phase shifts over a larger range of positron momenta. As expected, at large projectile energies, the scattering phase shift tends to zero. Note also that the phase shift is negative at all energies. This is a consequence of the positron–atom interaction being repulsive in the frozen-target approximation.

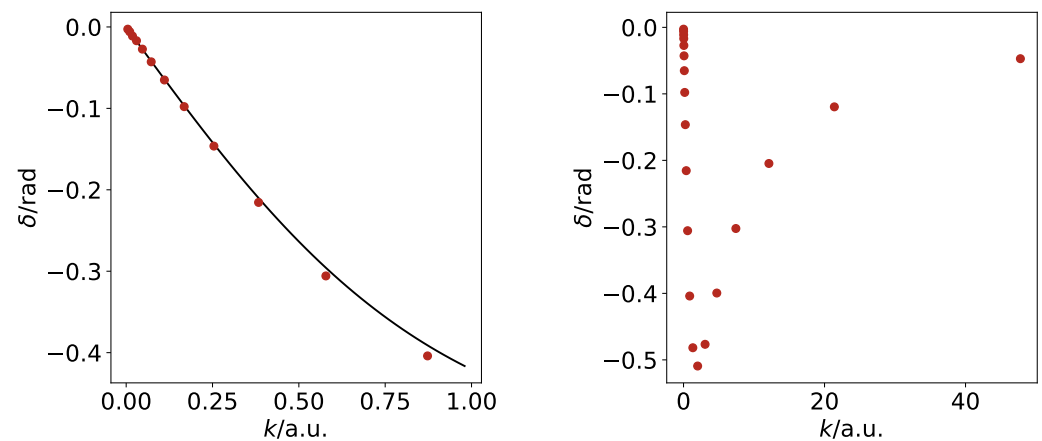


**Figure 4.** Positron–hydrogen s-wave scattering phase shifts in the static approximation calculated using a two-particle model (red circles), plotted over two contrasting ranges of  $k$ . The meaning of the black curve is the same as in Figure 3. Agreement with Figure 3 can be noted.

### 3.2.2. Variation of $\alpha$ : Radial Correlations.

To probe the effect of electron–positron radial correlations, the wavefunction is augmented by including extra terms with  $\alpha_i \neq 1$ . Physically, this adjustment allows the incident positron to cause displacement of the atomic electron in the radial direction due to the attraction between the two particles. Inclusion of a term, or several terms, in the wavefunction with  $\alpha_i = 0.5$  will facilitate this type of distortion. The wavefunction in this case is written as

$$\Psi(r_1, r_2) = \sum_{i=1}^N c_i \exp[-\alpha_i r_1 - \beta_i r_2]. \tag{38}$$

For now, the restriction on the  $\gamma_i$  parameters remains in place, in that  $\gamma_i = 0$  and the dependence of the wavefunction on the electron–positron distance is neglected. Note that this approximation corresponds to the so-called Temkin–Poet model that was used earlier to test electron–hydrogen and positron–hydrogen scattering [35].

Firstly, a single term is added with  $\alpha_i = 0.5$  and  $\beta_i = 0.4$ . This value of  $\beta_i$  is chosen because we expect radial correlations to be important when the positron is close to the hydrogen atom. At such distances, it is most likely to attract the electron sufficiently to cause significant distortion. Terms with  $\alpha_i = 0.5$  and a full range of  $\beta_i$  values are not immediately introduced because we aim to achieve good accuracy with as few correlation terms as possible. Hence, extra terms are introduced individually to test their importance: if a notable change in the phase shift is seen by adding a particular term, the term is retained and used in the basis. If not, the term is discarded and a different choice is made.

Phase shifts were obtained for various sets of parameters, using up to 20 additional terms. It was found that overall, the effect on the phase shift from adding these terms is small. In Figure 5, a set of results is displayed for a calculation with just three additional terms in the basis, which were found to generate a close-to-maximum shift from the frozen-target results (with  $\alpha_i = 0.5$  and  $\beta_i = 0.2, 0.4, 1.0$ ).

A comparison of Figure 5 with Figure 4 shows that the phase shifts have become slightly less negative due to the addition of the extra terms. This means that electron–positron correlations make the positron–atom interaction less repulsive than in the frozen-target case. However, the overall effect of allowing for the radial correlations between the electron and positron remains very small.

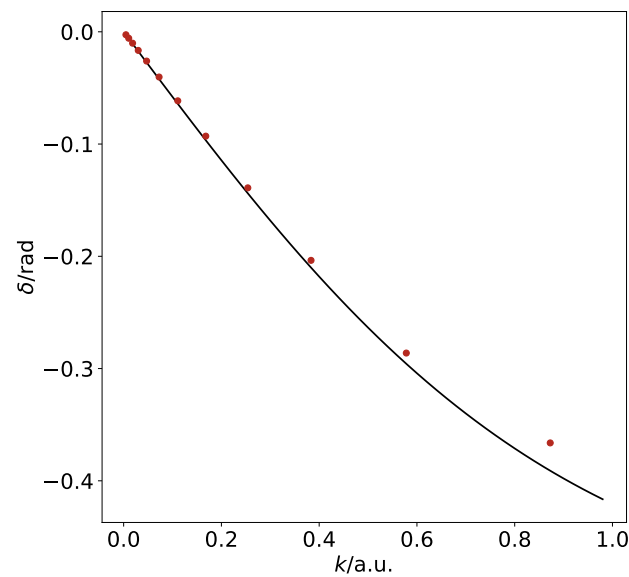


**Figure 5.** Phase shifts obtained by addition of three terms with  $\alpha_i \neq 1$  to the basis. Black line: numerical solution of the radial Schrödinger equation in the static potential of the hydrogen atom included for comparison.

### 3.2.3. Nonzero $\gamma$ : Effect of Angular Correlations.

In this section, the flexibility of the wavefunction is increased further by allowing for nonzero values of  $\gamma_i$ , so that the wavefunction takes the most general form

$$\Psi(r_1, r_2, r_{12}) = \sum_{i=1}^N c_i \exp(-\alpha_i r_1 - \beta_i r_2 + \gamma_i r_{12}). \tag{39}$$

The addition of  $r_{12}$ -dependence to the wavefunction allows for much stronger correlation between the positron and the electron. Physically, these terms account for effects such as virtual Ps formation and polarization of the atom by the positron. In particular, setting  $\gamma_i = -0.5$  corresponds to the ground-state Ps wavefunction, allowing the calculation to account for the effect of virtual positronium formation. Note that formation of “real”, free Ps is not possible in the chosen energy range, as the incident positron momenta are kept below the Ps formation threshold.

In general, terms with any values of  $\beta_i$  and  $\gamma_i$  may be used, provided that

$$\beta_i - \gamma_i > 0, \tag{40}$$

to ensure that  $\Psi(r_1, r_2, r_{12}) \rightarrow 0$  for  $r_2 \rightarrow \infty$ .

Taking all of this into consideration, an initial basis was set up identically to that in the frozen-target problem with all values of  $\gamma_i = 0$  and  $\alpha_i = 1$ . The nonzero  $\gamma_i$  terms were added one by one. Quasi-optimal values of the parameters for these extra terms were selected by completing the calculations for different sets of exponents and keeping the term which caused the largest upward change in the phase shifts overall. In the present approach, larger phase shifts are obtained when the energy eigenvalues  $E_n$  are lower relative to  $E_n^{(0)}$ . In a variational calculation, lower energy eigenvalues are obtained when better wavefunctions are used. Hence, it is correct to assume that the best possible choice of terms to add to the basis is that which yields the largest values for the phase shifts. Physically, including electron–positron correlations allows for positron attraction to the atom, increasing the value of the phase shift. Small adjustments are made to all three parameters near the optimum to ensure the best possible value of each parameter, correct to two decimal places.

For a single correlation term, the optimal values of  $\alpha$ ,  $\beta$  and  $\gamma$  were found to be  $\alpha = 0.80$ ,  $\beta = 0.04$  and  $\gamma = -0.54$ . Once the first term had been optimized, a second

was added. The values of the parameters for this term were also selected in the manner described above. With each additional term, an improvement (i.e., increase) in the phase shift values is seen.

This process of adding an individual term may be continued for as many terms as required to reach a desired level of accuracy. However, our aim was to achieve good accuracy using as few terms as possible. Hence, the process was terminated after including a maximum of nine additional terms, yielding a basis with a total of 29 functions.

Figure 6 is an overview of the phase shifts obtained using one, three, five and nine additional terms. These results are also shown in Table 1. Details of the parameters used in these calculations can be found in Appendix B. The results obtained here can be compared to the accurate phase shifts, such as those calculated by Schwartz [23] or, later, by Humberston et al. [24]. In Figure 6, the frozen-target phase shifts are also plotted as a lower bound, while the accurate results from a Kohn variational calculation by Humberston et al. [24] provide an upper bound. It is remarkable that including a single well-chosen correlation term with  $\alpha = 0.80$ ,  $\beta = 0.04$  and  $\gamma = -0.54$  provides about 80% of the increase in the phase shift with respect to the uncorrelated frozen-target result. Adding the next few correlation terms brings the variational phase shift to within 0.01 rad of the benchmark result.

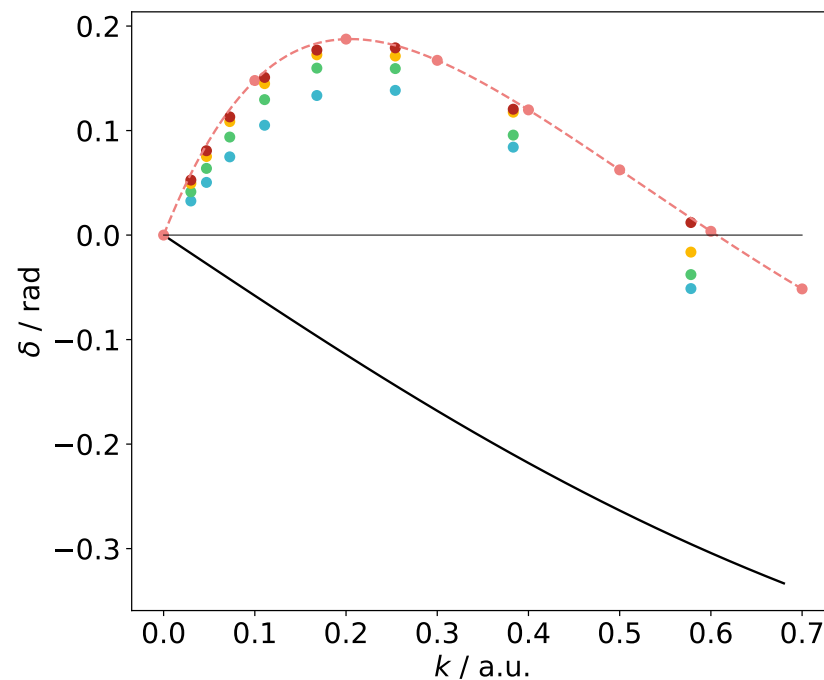


**Figure 6.** Positron–hydrogen *s*-wave scattering phase shifts obtained using various numbers of terms with  $\gamma_i \neq 0$  in the wavefunction (colored circles, blue: one term, green: three terms, yellow: five terms, red: nine terms). Details of the parameters used in each wavefunction can be found in Appendix B. Pink circles are the Kohn variational calculations of Humberston et al. [24], which are connected by the dashed line to guide the eye. The black solid line is the result of the frozen-target approximation.

In Figure 7, the final phase shifts obtained using all nine correlation (i.e., nonzero  $\gamma_i$ ) terms are displayed. Compared with an interpolation of the Kohn variational results of Humberston et al. [24], agreement is seen to within  $8 \times 10^{-3}$  rad. In Table 2, the present results obtained with nine correlation terms are shown alongside the results of Ref. [24] interpolated to the same momentum values. This level of agreement provides evidence that the method employed here is a valid approach to the positron scattering problem, and that it is possible to obtain good-quality scattering data from a bound-state-type calculation that contains only a small number of correlation terms in the wavefunction.

**Table 1.** Results from positron–hydrogen  $s$ -wave phase shift calculations with wavefunctions containing  $N_E = 1, 3, 5$  and  $9$  terms with nonzero  $\gamma_i$  to describe electron–positron correlations (see Appendix B). Phase shift values are shown for the first 11 eigenvalues  $E_n$ .

$N_E$	1		3		5		9	
$n$	$k/a.u.$	$\delta/rad$	$k/a.u.$	$\delta/rad$	$k/a.u.$	$\delta/rad$	$k/a.u.$	$\delta/rad$
1	0.0046	0.0049	0.0046	0.0063	0.0046	0.0075	0.0046	0.0082
2	0.0104	0.0115	0.0104	0.0145	0.0104	0.0176	0.0104	0.0189
3	0.0183	0.0201	0.0183	0.0257	0.0183	0.0307	0.0183	0.0334
4	0.0299	0.0326	0.0299	0.0415	0.0299	0.0494	0.0299	0.0526
5	0.0470	0.0504	0.0470	0.0638	0.0470	0.0752	0.0470	0.0807
6	0.0725	0.0748	0.0725	0.0938	0.0725	0.1086	0.0725	0.1130
7	0.1107	0.1051	0.1107	0.1296	0.1107	0.1449	0.1107	0.1509
8	0.1680	0.1335	0.1680	0.1597	0.1680	0.1725	0.1680	0.1770
9	0.2540	0.1384	0.2540	0.1593	0.2540	0.1713	0.2540	0.1791
10	0.3834	0.0841	0.3834	0.0957	0.3834	0.1176	0.3833	0.1204
11	0.5782	−0.0512	0.5782	−0.0378	0.5782	−0.0163	0.5781	0.0120

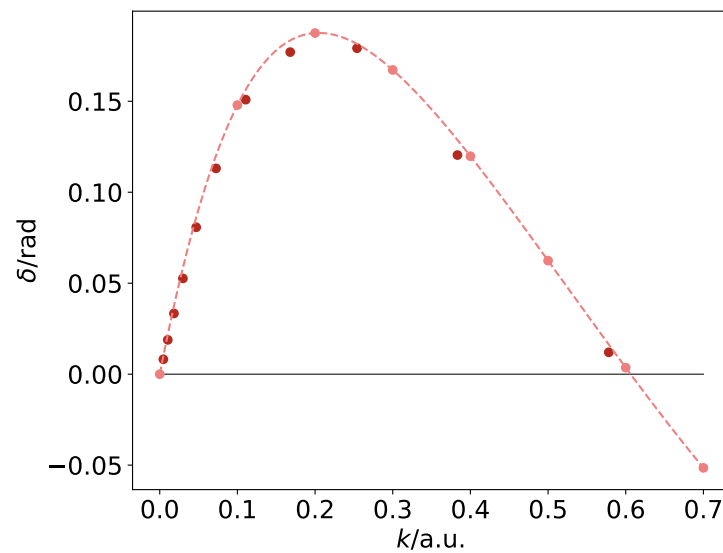


**Figure 7.** Positron–hydrogen  $s$ -wave scattering phase shifts obtained using nine nonzero  $\gamma_i$  terms in the wavefunction with various  $\alpha_i$ ,  $\beta_i$  and  $\gamma_i$  values (red circles). Details of the parameters used in this wavefunction can be found in Appendix B. Pink circles connected by the dashed line are calculations of Humberston et al. [24].

**Table 2.** Results from positron–hydrogen  $s$ -wave phase shift calculations with nine  $\gamma_i \neq 0$  terms in the wavefunction (see Appendix B) for the first 11 energy eigenvalues  $E_n$ . The phase shifts of Humberston et al. [24]  $\delta_H$  interpolated to the same values of  $k$  are also shown.

$n$	$k/a.u.$	$\delta/rad$	$\delta_H/rad$	Error/rad
1	0.0046	0.0082	0.0100	0.0018
2	0.0104	0.0189	0.0219	0.0030
3	0.0183	0.0334	0.0375	0.0041
4	0.0299	0.0526	0.0586	0.0059
5	0.0470	0.0807	0.0862	0.0055
6	0.0725	0.1130	0.1202	0.0071
7	0.1107	0.1509	0.1564	0.0055
8	0.1680	0.1770	0.1835	0.0065
9	0.2540	0.1791	0.1815	0.0024
10	0.3833	0.1204	0.1287	0.0083
11	0.5781	0.0120	0.0163	0.0043

#### 4. Calculation of the Annihilation Parameter

In this section, the quality of the variational wavefunctions constructed as described in Section 3 is probed by calculating the normalized annihilation rate,  $Z_{\text{eff}}$ .  $Z_{\text{eff}}$  is the effective number of electrons available to the positron for annihilation [36]. For a positron incident on the hydrogen atom, it is given by [13]:

$$Z_{\text{eff}} = \iint \delta(\mathbf{r}_1 - \mathbf{r}_2) |\Psi_k(\mathbf{r}_1, \mathbf{r}_2)|^2 d^3\mathbf{r}_1 d^3\mathbf{r}_2, \tag{41}$$

where the wavefunction is normalized to the incident positron plane wave, i.e.,  $\Psi_k(\mathbf{r}_1, \mathbf{r}_2) \simeq \psi_{1s}(\mathbf{r}_1) \exp(i\mathbf{k} \cdot \mathbf{r}_2)$ , or, for  $s$ -wave positron scattering,  $\Psi_k(\mathbf{r}_1, \mathbf{r}_2) \simeq \psi_{1s}(\mathbf{r}_1) \sin(kr_2 + \delta)/kr_2$ .

Carrying out the integration over  $\mathbf{r}_1$  and renaming  $\mathbf{r}_2 \equiv \mathbf{r}$  gives

$$Z_{\text{eff}} = \int |\Psi_k(\mathbf{r}, \mathbf{r})|^2 d^3\mathbf{r}. \tag{42}$$

In this integral,  $|\Psi_k(\mathbf{r}, \mathbf{r})|^2$  is the electron–positron contact density localized near the atom. Unlike the scattering phase shifts which characterize the wavefunction at large positron distances, the  $Z_{\text{eff}}$  parameter probes the wavefunction at small positron–atom separations. Here, the bound-state-type variational wavefunction  $\Psi$  is proportional to the true continuous spectrum wavefunction  $\Psi_k$ , i.e., we have

$$\Psi(\mathbf{r}_1, \mathbf{r}_2) = \frac{A}{\sqrt{4\pi}} \Psi_k(\mathbf{r}_1, \mathbf{r}_2), \tag{43}$$

where  $A$  is a normalization constant. For  $s$ -wave scattering, the normalization constant is obtained from the energy eigenvalue spectrum as (see Ref. [31] for details)

$$A^2 = \frac{2\sqrt{2E}}{\pi} \frac{dE}{dn}. \tag{44}$$

The wavefunctions  $\Psi$  generated by solving the generalized eigenvalue problem (as outlined in Section 3) are automatically normalized to unity. Hence, to achieve the correct normalization, these wavefunctions must be divided by  $A$  when calculating  $Z_{\text{eff}}$  from (42). The value of  $A$  is calculated for each eigenfunction by substituting the corresponding energy eigenvalue into (44). The derivative  $dE/dn$  is evaluated using the function  $n = g(\ln E)$  from Section 3 and the fact that

$$\frac{dE}{dn} = E \frac{d \ln E}{dn}. \tag{45}$$

This facilitates a more accurate calculation of the derivative than that obtained by directly calculating  $dE/dn$ .

The annihilation parameter is first calculated in the frozen-target approximation, after which the two-particle problem is considered to include electron–positron correlations.

##### 4.1. One-Particle Calculation

In the one-particle frozen-target calculation, the wavefunction only depends on the positron radial coordinate  $r$ . The trial wavefunction (11) is employed for this calculation. The  $c_i$  values calculated previously are used again here, but each eigenfunction is divided by  $A$  to fulfill the normalization condition (43).

In Figure 8, the eigenfunctions obtained using the present method are divided by  $A$  and multiplied by  $\sqrt{k/\pi}$ , and they are compared to the true continuous-spectrum radial function  $P_k(r)$  obtained by solving the radial Schrödinger equation [33] and normalized as

$$P_k(r) \simeq \frac{\sin(kr + \delta)}{\sqrt{\pi k}}. \tag{46}$$

For small  $r$ , these were found to be in good agreement. As the energy eigenvalues increase, the range of  $r$  over which the wavefunctions closely match decreases. However, there is always a very good match at  $r \sim 1$  a.u., which dominates in the calculation of  $Z_{\text{eff}}$ .

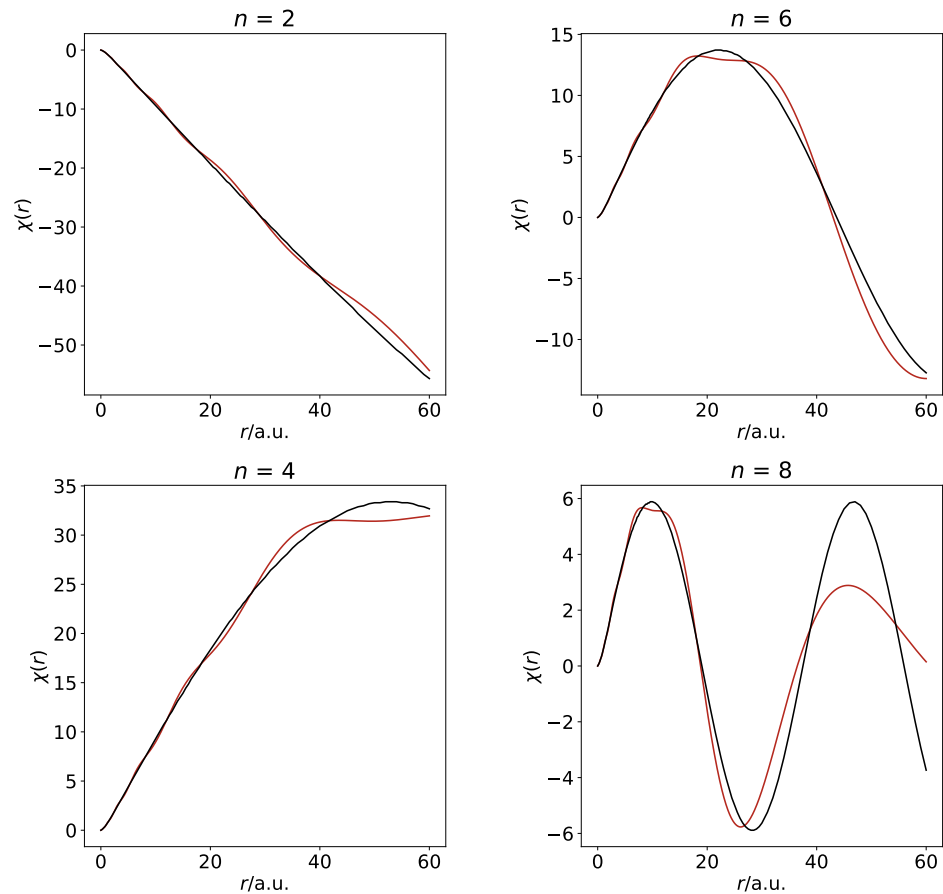


**Figure 8.** Eigenfunctions obtained from solving the generalized eigenvalue problem (6) in the static approximation (red) and those obtained using the atomic codes [33] (black) for  $n = 2, 4, 6$  and  $8$ .

The following integral is used to evaluate  $Z_{\text{eff}}$  in this problem [13]:

$$Z_{\text{eff}} = \frac{1}{A^2} \int_0^\infty P_{1s}^2(r) \Psi^2(r) r^{-2} dr, \tag{47}$$

where  $P_{1s}(r) = 2re^{-r}$  is the ground-state radial wavefunction of the hydrogen atom. Substituting (11) into (47) gives the following expression for the annihilation parameter:

$$Z_{\text{eff}} = \frac{8}{A^2} \sum_{i,j=1}^N \frac{c_i c_j}{(2 + \alpha_i + \alpha_j)^3}. \tag{48}$$

Figure 9 shows the corresponding frozen-target  $Z_{\text{eff}}$  values and compares them with those obtained using true continuous-spectrum positron states in the same approximation [13,33]. Apart from some “noise” related to inaccuracies in the calculation of the normalization constant  $A$  at low energies, there is a good general agreement between the two sets of results.

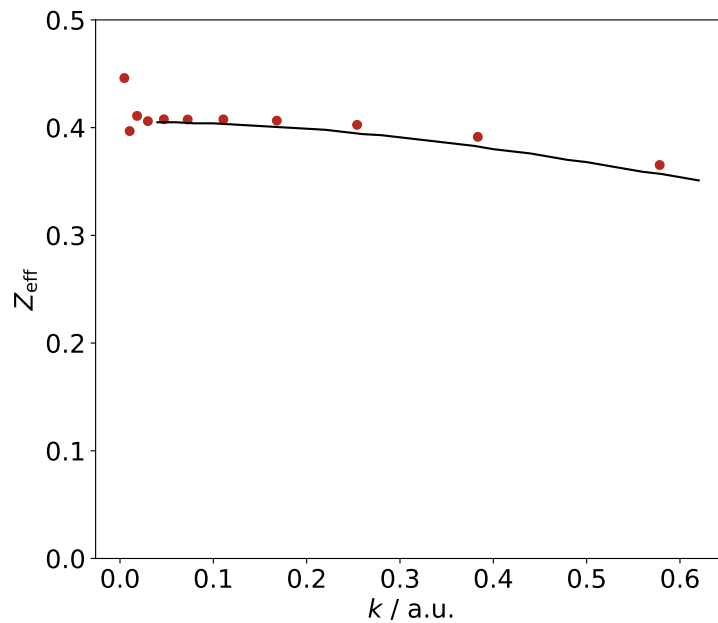


**Figure 9.** Red circles: values of  $Z_{\text{eff}}$  obtained in the one-particle model with variational wavefunctions from (48). Black line:  $Z_{\text{eff}}$  data obtained for the frozen-target model from atomic codes [13,33].

#### 4.2. Two-Particle Calculation

In this section, the annihilation parameter is calculated for the two-particle problem. Firstly, the frozen-target results are reproduced by the two-particle code, using a wavefunction with the form of (39) with all  $\alpha_i = 1$  and  $\gamma_i = 0$ . After verifying that the results match those from the one-particle calculation, these restrictions on the  $\alpha_i$  and  $\gamma_i$  values are lifted, and the full correlated wavefunction is used, subject to (40). Here, it is noted that  $r_{12} = 0$  in the  $Z_{\text{eff}}$  calculation, so  $\exp(\gamma_i r_{12}) = 1$  for each of the  $\gamma_i$ . In addition,  $r_1 = r_2 \equiv r$  is required, and the wavefunction takes the form

$$\Psi(r, r, 0) = \sum_{i=1}^N c_i \exp[-(\alpha_i + \beta_i)r]. \tag{49}$$

As before, the  $c_i$  coefficients are calculated such that the eigenfunctions are normalized to unity. Hence, the normalization must be corrected to satisfy (43) using the value of  $A$  for each eigenfunction.

In this case, evaluation of the integral (42) with the wavefunction (49) yields the following expression for  $Z_{\text{eff}}$ :

$$Z_{\text{eff}} = \frac{16\pi^2}{A^2} \int_0^\infty |\Psi(r, r, 0)|^2 r^2 dr = \frac{32\pi^2}{A^2} \sum_{i,j=1}^N \frac{c_i c_j}{(\alpha_i + \alpha_j + \beta_i + \beta_j)^3}. \tag{50}$$

The coefficients  $c_i$  in this calculation differ from those in the one-particle calculation by a factor of  $1/2\pi$ . Taking this into account, the equivalence of the one- and two-particle results can be verified by setting  $\alpha_i = \alpha_j = 1$  in (50) to recover the result from the frozen-target approximation (48). Here, however, the focus is on including terms in the wavefunction to describe electron–positron correlations.

When incorporating correlation terms, the same sets of  $\alpha_i$ ,  $\beta_i$  and  $\gamma_i$  parameters are used in the basis as for the phase shift calculations in Section 3.2.3 (the values of which are listed in Appendix B). The accuracy of the  $Z_{\text{eff}}$  calculation does not increase monotonically with the number of correlation terms included the wavefunction, unlike the case of the phase shifts determined by the energy eigenvalues alone. This is shown in Figure 10, where the overall results obtained using one correlation term are more accurate than those obtained using three correlation terms. However, the most accurate set of values

was obtained for the wavefunction with the maximum (nine) correlation terms included. The  $Z_{\text{eff}}$  values from [26] are used as benchmark values to evaluate the accuracy of our calculation. The results from the final calculation are displayed in Table 3 alongside those from [26] interpolated to the same values of momentum.

**Table 3.**  $Z_{\text{eff}}$  values obtained using a wavefunction with nine nonzero  $\gamma_i$  terms (Appendix B) to describe electron–positron correlations and the benchmark results from [26] ( $Z_{\text{eff,H}}$ ) interpolated to the same values of momentum.

$k/\text{a.u.}$	$Z_{\text{eff}}$	$Z_{\text{eff,H}}$	Error
0.0046	9.2538	9.6013	0.3475
0.0104	8.1989	9.4644	1.2655
0.0183	8.4351	9.2767	0.8416
0.0299	8.2262	9.0083	0.7821
0.0470	8.0325	8.6212	0.5887
0.0725	7.6456	8.0667	0.4211
0.1107	6.9813	7.2876	0.3063
0.1680	6.0719	6.2319	0.1600
0.2540	4.8017	4.8951	0.0934
0.3833	3.6024	3.4371	−0.1653
0.5781	2.0695	2.3833	0.3138

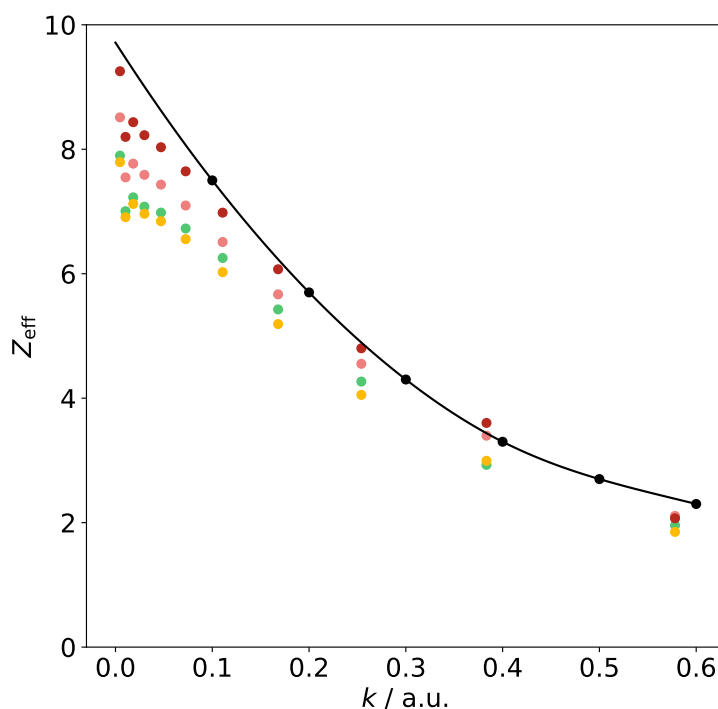


**Figure 10.**  $Z_{\text{eff}}$  values obtained in the two-particle model using one (green), three (yellow), five (pink) and nine (red) terms in the wavefunction to describe correlations between the electron and positron. Black circles and line: results from [26] and their interpolation using cubic splines.

Overall, good agreement between our results and the benchmark values is found in the range  $k = 0.1\text{--}0.6$  a.u. using a trial wavefunction with nine nonzero  $\gamma_i$  terms. Apart from two data points, the accuracy of our variational calculation is better than 10%, which is evidence of the good quality of the wavefunction that includes only a small number of correlation terms.

### 5. Conclusions

The variational method was explored as a means of studying positron–hydrogen scattering and annihilation using square-integrable trial wavefunctions. By setting up and solving a generalized eigenvalue problem, *s*-wave elastic phase shifts and  $Z_{\text{eff}}$  values for the positron–hydrogen system were obtained in good agreement with benchmark values. Importantly, this was achieved using only a small number of correlation terms in the trial wavefunction, indicating that processes such as virtual positronium formation and polarization of the hydrogen atom can be accounted for using this approach.

Looking forward, this method could facilitate the study of more complex interactions, such as the interaction of positrons with molecules. The key benefit of our approach is the small number of terms required to describe strong electron–positron correlations, meaning that the method is quite economical. To improve upon the current approach, a formal optimization of the trial wavefunction parameters could be performed to increase the accuracy of the calculation. With such a process in place, it would become possible to carry out more complex calculations efficiently.

**Author Contributions:** Methodology, G.G. and S.G.; software, S.G.; writing, G.G. and S.G.; supervision, G.G. All authors have read and agreed to the published version of the manuscript.

**Funding:** This research received no external funding.

**Data Availability Statement:** All data are available from the authors upon request.

**Conflicts of Interest:** The authors declare no conflict of interest.

### Appendix A. Standard Integrals

This appendix contains results for the six standard integrals employed throughout our calculations. These are evaluated using the elliptic coordinate system:  $s = r_1 + r_2$ ,  $t = r_1 - r_2$  and  $u = r_{12}$ :

$$\begin{aligned} \tilde{I}_1(a, b, g) &= \pi^2 \int_0^\infty ds e^{-2as} \int_0^s du ue^{2bu} \int_{-u}^u dt e^{-2gt} (s^2 - t^2) \\ &= \pi^2 \frac{8a^3 - 13a^2b + 6ab^2 - b^3 + bg^2}{8a^3((a - b)^2 - g^2)^3}, \end{aligned} \tag{A1}$$

$$\begin{aligned} \tilde{I}_2(a, b, g) &= \pi^2 \int_0^\infty ds se^{-2as} \int_0^s du e^{2bu} \int_{-u}^u dt e^{-2gt} (u^2 - t^2) \\ &= \pi^2 \frac{5a^2 - 6ab + b^2 - g^2}{8a^2((a - b)^2 - g^2)^3}, \end{aligned} \tag{A2}$$

$$\begin{aligned} \tilde{I}_3(a, b, g) &= \pi^2 \int_0^\infty ds e^{-2as} \int_0^s du (s^2 - u^2)e^{2bu} \int_{-u}^u dt te^{-2gt} \\ &= \pi^2 g \frac{(-5a^2 + 6ab - b^2 + g^2)}{8a^3((a - b)^2 - g^2)^3}, \end{aligned} \tag{A3}$$

$$\begin{aligned} \tilde{J}_1(a, b, g) &= \pi^2 \int_0^\infty ds se^{-2as} \int_0^s du ue^{2bu} \int_{-u}^u dt e^{-2gt} \\ &= \pi^2 \frac{(a - b)^2(4a - b)g + bg^3}{8a^2g((a - b)^2 - g^2)^3}, \end{aligned} \tag{A4}$$

$$\begin{aligned} \tilde{J}_2(a, b, g) &= \pi^2 \int_0^\infty ds e^{-2as} \int_0^s du e^{2bu} \int_{-u}^u dt e^{-2gt}(s^2 - t^2) \\ &= -\pi^2 \frac{-5a^2 + 4ab - b^2 + g^2}{8a^3((a - b)^2 - g^2)^2}, \end{aligned} \tag{A5}$$

$$\begin{aligned} \tilde{J}_3(a, b, g) &= \pi^2 \int_0^\infty ds e^{-2as} \int_0^s du ue^{2bu} \int_{-u}^u dt te^{-2gt} \\ &= -\pi^2 \frac{(a - b)g}{2a((a - b)^2 - g^2)^3}. \end{aligned} \tag{A6}$$

### Appendix B. Parameters for Positron-Scattering Wavefunction Bases

The positron–hydrogen wavefunctions used in Sections 3.2 and 4.2 all contain the 20 basis functions defined by (13) with  $n = 20$ ,  $\zeta = 1.5$  and  $\beta_1 = 0.01$  (where all  $\alpha_i = 1$  and  $\gamma_i = 0$ ). Additional terms with varying  $\alpha_i$  and nonzero  $\gamma_i$  values were then incorporated to account for electron–positron correlations. The table below contains the sets of quasi-optimal values for the parameters obtained using the method described in Section 3.2. These values are displayed for wavefunctions containing one, three, five and nine terms with nonzero  $\gamma_i$  where  $N_E$  denotes the number of nonzero  $\gamma_i$  terms.

**Table A1.** Parameters used for the electron–positron correlation terms, i.e, terms with nonzero  $\gamma_i$ , in positron–hydrogen wavefunctions with  $N_E = 1, 3, 5$  and 9 such terms.

$N_E$	$\alpha$	$\beta$	$\gamma$	$N_E$	$\alpha$	$\beta$	$\gamma$
1	0.80	0.04	−0.54	9	0.79	0.06	−0.53
3	0.80	0.05	−0.56		0.99	0.40	0.11
	0.88	0.45	0.10		1.00	0.14	−0.03
	0.97	0.28	−0.46		0.40	0.04	−0.38
5	0.80	0.05	−0.54		0.85	0.88	−0.38
	0.98	0.46	0.06		0.29	0.40	−0.70
	0.99	0.14	−0.11		0.85	0.50	−0.27
	0.45	0.12	−0.67		0.84	−0.20	−0.65
	0.86	0.93	−0.31		0.99	0.67	−0.01

### Notes

- Atomic units are used throughout (in which  $e = m = \hbar = 1$ , where  $e$  is the elementary charge and  $m$  is the electron or positron mass).
- For a state with a zero total angular momentum, the wavefunction is spherically symmetric, so there is no dependence on the directions of  $r_1$  and  $r_2$ , except the angle between them, i.e., dependence on  $r_{12}$ .

### References

- Chua, S.; Groves, A. *Biomedical Imaging Applications and Advances*; Woodhead Publishing: Cambridge, UK, 2014.
- Tuomisto, F.; Makkonen, I. Defect identification in semiconductors with positron annihilation: Experiment and theory. *Rev. Mod. Phys.* **2013**, *85*, 1583–1631. [[CrossRef](#)]
- Ishida, A.; Namba, T.; Asai, S.; Kobayashi, T.; Saito, H.; Yoshida, M.; Tanaka, K.; Yamamoto, A. New precision measurement of hyperfine splitting of positronium. *Phys. Lett. B* **2014**, *734*, 338. [[CrossRef](#)]
- Ahmadi, M.; Alves, B.X.R.; Baker, C.J.; Bertsche, W.; Capra, A.; Carruth, C.; Cesar, C.L.; Charlton, M.; Cohen, S.; Collister, R.; et al. Investigation of the fine structure of antihydrogen. *Nature* **2020**, *578*, 375–380. [[CrossRef](#)]
- Dirac, P.A.M. Quantised Singularities in the Electromagnetic Field. *Proc. R. Soc. Lond. Ser. A* **1931**, *133*, 60–72. [[CrossRef](#)]
- Anderson, C.D. The positive electron. *Phys. Rev.* **1932**, *43*, 491–494. [[CrossRef](#)]
- Surko, C.M.; Gribakin, G.F.; Buckman, S.J. Low-energy positron interactions with atoms and molecules. *J. Phys. B* **2005**, *38*, R57–R126. [[CrossRef](#)]
- Amusia, M.Y.; Cherepkov, N.A.; Chernysheva, L.V.; Shapiro, S.G. Elastic scattering of slow positrons by helium. *J. Phys. B* **1976**, *9*, L531–L534. [[CrossRef](#)]
- Amusia, M.Y.; Dolmatov, V.K.; Chernysheva, L.V. Positron elastic scattering by a semifilled-shell atom. *J. Phys. B* **2021**, *54*, 185003. [[CrossRef](#)]

10. Gribakin, G.F.; King, W.A. The effect of virtual positronium formation on positron-atom scattering. *J. Phys. B* **1994**, *27*, 2639–2645. [[CrossRef](#)]
11. Dzuba, V.A.; Flambaum, V.V.; Gribakin, G.F.; King, W.A. Bound states of positrons and neutral atoms. *Phys. Rev. A* **1995**, *52*, 4541. [[CrossRef](#)]
12. Dzuba, V.A.; Flambaum, V.V.; Gribakin, G.F.; King, W.A. Many-body calculations of positron scattering and annihilation from noble-gas atoms. *J. Phys. B* **1996**, *29*, 3151. [[CrossRef](#)]
13. Gribakin, G.F.; Ludlow, J. Many-body theory of positron-atom interactions. *Phys. Rev. A* **2004**, *70*, 032720. [[CrossRef](#)]
14. Green, D.G.; Ludlow, J.A.; Gribakin, G.F. Positron scattering and annihilation on noble-gas atoms. *Phys. Rev. A* **2014**, *90*, 032712. [[CrossRef](#)]
15. Hofierka, J.; Cunningham, B.; Rawlins, C.M.; Patterson, C.H.; Green, D.G. Many-body theory of positron binding to polyatomic molecules. *Nature* **2022**, *606*, 688–693. [[CrossRef](#)] [[PubMed](#)]
16. Bray, I.; Stelbovics, A.T. Convergent close-coupling calculations of low-energy positron–atomic-hydrogen scattering. *Phys. Rev. A* **1993**, *48*, 4787–4789. [[CrossRef](#)]
17. Mitroy, J.; Bromley, M.W.J. Convergence of configuration-interaction single-center calculations of positron-atom interactions. *Phys. Rev. A* **2006**, *73*, 052712. [[CrossRef](#)]
18. Kadyrov, A.S.; Bray, I. Two-center convergent close-coupling approach to positron-hydrogen collisions. *Phys. Rev. A* **2002**, *66*, 012710. [[CrossRef](#)]
19. Humberston, J.; Van Reeth, P. Annihilation in low energy positron-helium scattering. *Nucl. Instrum. Methods Phys. Res. B* **1998**, *143*, 127–134. [[CrossRef](#)]
20. Reeth, P.V.; Humberston, J.W. Elastic scattering and positronium formation in low-energy positron-helium collisions. *J. Phys. B* **1999**, *32*, 3651–3667. [[CrossRef](#)]
21. Germano, J.S.E.; Lima, M.A.P. Schwinger multichannel method for positron-molecule scattering. *Phys. Rev. A* **1993**, *47*, 3976–3982. [[CrossRef](#)]
22. da Silva, E.P.; Germano, J.S.E.; Lima, M.A.P. Annihilation Dynamics of Positrons in Molecular Environments: Theoretical Study of Low-Energy Positron-  $C_2H_4$  Scattering. *Phys. Rev. Lett.* **1996**, *77*, 1028–1031. [[CrossRef](#)] [[PubMed](#)]
23. Schwartz, C. Electron Scattering from Hydrogen. *Phys. Rev.* **1961**, *124*, 1468–1471. [[CrossRef](#)]
24. Humberston, J.W.; Reeth, P.V.; Watts, M.S.T.; Meyerhof, W.E. Positron-hydrogen scattering in the vicinity of the positronium formation threshold. *J. Phys. B* **1997**, *30*, 2477–2493. [[CrossRef](#)]
25. Bhatia, A.K. Positron-Hydrogen Scattering, Annihilation, and Positronium Formation. *Atoms* **2016**, *4*, 27. [[CrossRef](#)]
26. Humberston, J.W.; Wallace, J.B.G. The elastic scattering of positrons by atomic hydrogen. *J. Phys. B* **1972**, *5*, 1138–1148. [[CrossRef](#)]
27. Ghosh, A.; Sil, N.; Mandal, P. Positron-atom and positron-molecule collisions. *Phys. Rep.* **1982**, *87*, 313–406. [[CrossRef](#)]
28. Gien, T.T. Coupled-state calculations of positron-hydrogen scattering. *Phys. Rev. A* **1997**, *56*, 1332–1337. [[CrossRef](#)]
29. Ghoshal, A.; Mandal, P. Correlated dipole-polarized basis in Schwinger’s principle for elastic positron-hydrogen collisions. *Phys. Rev. A* **2005**, *72*, 042709. [[CrossRef](#)]
30. Available online: <https://docs.scipy.org/doc/scipy/reference/generated/scipy.linalg.eigh.html> (accessed on 3 February 2021).
31. Swann, A.R.; Gribakin, G.F. Model-potential calculations of positron binding, scattering, and annihilation for atoms and small molecules using a Gaussian basis. *Phys. Rev. A* **2020**, *101*, 022702. [[CrossRef](#)]
32. Landau, L.D.; Lifshitz, E.M. *Quantum Mechanics*, 3rd ed.; Pergamon: Oxford, UK, 1977.
33. Amusia, M.Y.; Chernysheva, L.V. *Computation of Atomic Processes: A Handbook for the ATOM Programs*; Institute of Physics Publishing: Bristol, UK, 1997.
34. Hylleraas, E.A. Über den Grundzustand des Heliumatoms. *Z. Phys.* **1928**, *48*, 469–494. [[CrossRef](#)]
35. Kadyrov, A.S.; Bray, I.; Stelbovics, A.T. Near-Threshold Positron-Impact Ionization of Atomic Hydrogen. *Phys. Rev. Lett.* **2007**, *98*, 263202. [[CrossRef](#)] [[PubMed](#)]
36. Fraser, P. Positrons and Positronium in Gases. In *Advances in Atomic and Molecular Physics*; Academic Press: New York, NY, USA, 1968; Volume 4, pp. 63–107. [[CrossRef](#)]